High-Resolution Topographic Imaging of Environmentally Responsive, Elastin-Mimetic Hydrogels

R. Andrew McMillan,‡ Kevin L. Caran,† Robert P. Apkarian,† and Vincent P. Conticello*,‡

Integrated Microscopy & Microanalytical Facility and Department of Chemistry, Emory University, Atlanta, Georgia 30322

Received July 13, 1999
Revised Manuscript Received November 2, 1999

Biocompatible polymer hydrogels are extensively employed in biomedical and pharmaceutical applications as prosthetic devices, drug delivery agents, and matrices for cell encapsulation and tissue engineering.[1] The three-dimensional architecture of the polymer network has an important influence on the performance of these materials as it mediates polymer−solvent interactions and defines biomedically important materials properties including the solute permeability, the equilibrium swelling ratio, and the viscoelasticity of the gel.[2] However, few analytical techniques are currently available that can directly interrogate the morphology of polymer hydrogels under conditions that approximate the functional environment of the materials. Recently, high-resolution topographic images have been obtained on biomolecules and intact cells under native, hydrated conditions using a combination of extremely rapid cryoimmobilization and in-lens field emission scanning electron microscopy at low temperature.[3] We report herein the use of these techniques to investigate the morphological changes that occur in the microstructure of an environmentally responsive protein polymer and hydrogel upon passage through the phase transition.

We have previously described the biosynthesis and characterization of an elastin-mimetic protein polymer of uniform and defined length, poly(**Lys-25**), based upon the repeat sequence [(Val-Pro-Gly-Val-Gly)$_4$(Val-Pro-Gly-Lys-Gly)], **1**.[4,5] Poly(**Lys-25**) undergoes a temperature-dependent phase transition in aqueous solution in analogy to soluble elastin derivatives and chemosynthetic elastin-mimetic polymers.[6] In this process, phase separation of the polypeptide from aqueous solution occurs above a lower critical solution temperature T_t.[7] The position of the phase transition for poly(**Lys-25**) depends on the pH of the solution due to proton-transfer equilibria involving the lysine residues within the repeats. The transition temperature of poly(**Lys-25**) shifts from 28 °C in 0.1 N NaOH with the lysine residues in the free amine state to 75 °C at neutral pH with the lysine residues in the ammonium ion state. The ϵ-amino groups of the lysine residues in poly(**Lys-25**) can be selectively cross-linked *under controllable conditions* to afford a synthetic hydrogel that mimics the responsive properties of native elastic fiber and chemosynthetic elastin-mimetic networks (Figure 1).[8,9] This elastin-mimetic hydrogel undergoes a discontinuous volume transition as the temperature approaches the phase boundary with a transition midpoint at approximately 35 °C in unbuffered water at neutral pH. The position of this phase transition is shifted approximately 40 °C lower than that of aqueous solutions of poly(**Lys-25**) under identical conditions due to conversion of the protonated ϵ-amino groups of the lysine side chains into less polar, uncharged amide groups during the cross-linking reaction.

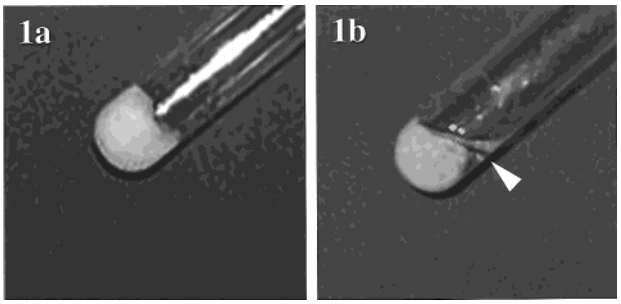

Figure 1. Photographic images of an elastin-mimetic hydrogel in the expanded (a) and collapsed (b) forms at temperatures below (4 °C) and above (40 °C) the phase transition, respectively. Both gels have an opalescent appearance due to microscopic phase separation (microsyneresis) during the cross-linking reaction.[24] Macroscopic phase separation (macrosyneresis) can be detected in the gel above the transition temperature by the appearance of a separate aqueous phase (arrowhead).

The structural rearrangements that occur in the hydrogel as a consequence of the phase transition should provide direct insight into the relationship between supramolecular organization and macroscopic responsive behavior in elastin-mimetic materials. Previous investigations into the morphology of these elastin-mimetic hydrogels employed a critical point drying technique for preparation of the specimens prior to image acquisition.[9] A beaded, filamentous microstructure was observed for these specimens that was reminiscent of the architecture of native elastic fiber and synthetic elastin networks. However, the feature sizes of the filaments were 2 orders of magnitude larger than those observed for similar elastin polypeptides.[10−12] Moreover, the hydration sphere of the polypeptide was displaced during the fixation, which precluded an investigation of the morphological changes induced by the phase transition. Cryoscopic high-resolution scanning electron microscopy was employed to investigate the structural rearrangements that accompany the phase transition in the hydrogel *under conditions that approximate its functional environment*.[13] The expanded and collapsed states of the water-swollen, elastin-mimetic hydrogel were kinetically trapped by rapid cryoimmobilization after equilibration below (4 °C) and above (40 °C) the phase transition, respectively. Profound differences in morphology were observed between the expanded, low-temperature hydrogel (Figure 2) and in the collapsed, high-temperature hydrogel (Figure 3), although both specimens retained the microscopic phase separation (microsyneresis) that was previously observed in the dried hydrogels.[9]

The morphology of the expanded, water-swollen gel at low magnification consisted of an interconnected network of dendritic leaflets (Figure 2a) in which the extension across the surface of a leaflet was significantly

* To whom correspondence should be addressed at vcontic@emory.edu.
† Integrated Microscopy & Microanalytical Facility, Emory University.
‡ Department of Chemistry, Emory University.

10.1021/ma991119z CCC: $18.00
Published on Web 12/03/1999

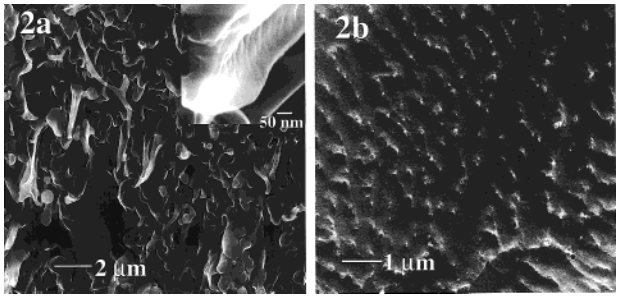

Figure 2. Cryo-HRSEM images of an elastin-mimetic hydrogel in its low-temperature, expanded state at intermediate magnification. The fracture surfaces of the specimens are depicted parallel (a) and perpendicular (b) to the leaflet surface. At high primary magnification (part a, inset), rough striations were observed on the surface of the leaflets at intervals of approximately 10 nm.

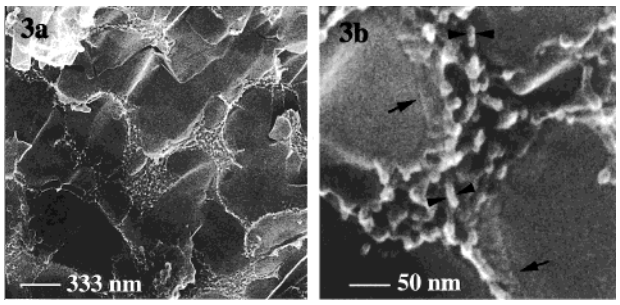

Figure 3. Cryo-HRSEM images of the fracture surface of an elastin-mimetic hydrogel in the high temperature, collapsed state at intermediate (a) and high (b) primary magnification, respectively. Note the 7 nm wide filaments (arrowheads) in the interior of the polymer-rich zone and the 2 nm wide interface (arrows) between the vitreous ice and gel phases in part b.

greater than its thickness. On alternate fracture surfaces, the leaflets could be observed in profile (Figure 2b), which provided a determination of their thickness (approximately 20−30 nm). Interestingly, vitreous ice was not detected in images in which the fracture surface is roughly parallel to the leaflet surface (Figure 2a), but it was observed for fracture surfaces that are perpendicular to the leaflet surface (Figure 2b). In the former case, the protein gel became separated from the vitrified solvent during the cryofracture operation. At high primary magnification, a series of rough striations was occasionally observed on the surface of the leaflets at an approximate spacing of 10 nm between the features (Figure 2a inset). The morphology of the expanded gel bore a striking resemblance to that observed for thin filaments and broad ribbonlike fibers obtained from electro-spinning of concentrated solutions of poly(**Lys-25**) at temperatures below the coacervation point.[14] This morphological similarity between elastin-mimetic fibers and swollen hydrogels derived from poly(**Lys-25**) implied a common underlying structure for these materials below the phase transition (vide infra).

The morphology of the elastin-mimetic hydrogel in its collapsed state differed distinctly from the hydrogel equilibrated below the phase transition. At intermediate magnification (Figure 3a), the collapsed polymer formed a honeycomb network around lakes of vitreous ice at the fracture surface. The interior of the polymer-rich zones comprised a network of beaded filaments, which could be more clearly discerned at high primary magnification (Figure 3b). This beaded, filamentous network closely resembled the morphology typically observed in

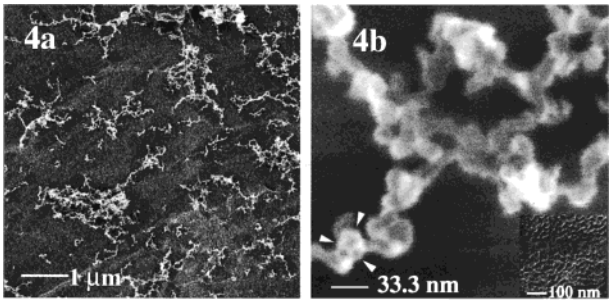

Figure 4. Cryo-HRSEM images of a coacervate of poly(**Lys-25**) at low (a) and high (b) primary magnification, respectively. A solution of poly(**Lys-25**) (1 mg/mL) in 0.1 N NaOH was heated at 40 °C to produce the coacervate, which was trapped by plunging the specimen into liquid ethane.[13] Notice the individual beads within a supercoiled filament (arrowheads) in part b. The individual filaments coalesced into a densely packed matrix at later stages of the coacervation process (part b, inset).

specimens of native elastic fiber and tropoelastin coacervates.[10−12] The filaments consisted of regularly spaced globules, ranging from 7 to 10 nm in diameter that aggregated lateral to the fracture plane and formed a densely packed matrix. In addition, a border zone was observed between the interior of the polymer-rich region and the vitreous ice. This shoreline region consisted of a narrow interface, approximately 2 nm in width, and a fine fibrillar lacework that extended approximately 20 nm into the polymer-rich zone. The extended morphology that was observed in the border region approximated the leaflet morphology of the expanded hydrogel, perhaps because interfacial confinement forced a polymer−solvent interaction similar to the latter system.

The morphology of the collapsed state of elastin-mimetic protein hydrogel can be compared with that of a coacervate of the non-cross-linked polymer precursor poly(**Lys-25**) imaged under nearly identical conditions (Figure 4). At an early stage of the coacervation process, individual wormlike filaments of the protein polymer separated from the surrounding vitreous ice and were observed at the fracture surface (Figure 4a). At high primary magnification, HRSEM images revealed wormlike, beaded filaments in which the smallest discernible features within the filaments were approximately 8 nm in diameter (Figure 4b). This filamentous morphology paralleled the topography observed in the interior of the polymer-rich islets of the collapsed hydrogel. The filaments of the nascent coacervate formed supercoiled structures in aqueous solution (Figure 4b), which implied a flexible structure as expected based on the elastomeric character of elastin. At later stages of assembly, the individual filaments aggregated into monolithic structures in which the topography was consistent with a close-packed arrangement of beaded filaments approximately 20 nm in diameter (Figure 4b inset). A similar self-organization process was observed during the coacervation of tropoelastin in vitro, in which 5−7 nm wide filaments occurred in the initial stage of the assembly process.[10,15] These filaments aggregated into bundles and coalesced into a three-dimensional beaded network that resembled the structure of native elastic fiber. The consistent observation of a beaded filamentous structure among diverse elastin-mimetic protein polymers, hydrogels, and native elastin derivatives implied a common determinative structural inter-

action in these biomaterials above the transition temperature.

The differences in microstructure observed between the expanded and collapsed states of the elastin-mimetic hydrogel reinforce the hypothesis that a structural rearrangement occurs in the polypeptide during the phase transition. This microstructural reorganization coincides with the development of elastomeric restoring force in the coacervate, which underlies the tensile properties of elastin that define its physiological role.[16] Urry et al., have extensively characterized the secondary structures of a series of chemosynthetic elastin-mimetic protein polymers [(Val-Pro-Gly-Xaa-Gly)$_n$].[17−20] These investigations concluded that the local conformation of the polypeptide chain undergoes reversible conversion from a random coil to a type II β-turn as the temperature approaches the coacervation point. Recent temperature-dependent circular dichroism studies of oligopeptide models of the elastin repeat indicated that the pentapeptide repeat (Val-Pro-Gly-Val-Gly) is the minimum viscoelastic unit in the polymer and that individual pentapeptides adopted the β-turn conformation independently as the temperature approached the transition point.[21] These results correlate well with elastic and quasi-elastic light scattering studies of [(Val-Pro-Gly-Val-Gly)$_n$] in aqueous solution, which suggested that the polymer behaved as a coil of effective polymer segments—corresponding to the individual β-turn units—near the coacervation point.[7] This conformational transition in elastin-mimetic polypeptides is commensurate with the microstructural reorganization that was observed in the topographic images of the hydrogel under frozen, hydrated conditions although the correspondence between local and global polypeptide structural features has not been unequivocally established.

To our knowledge, these results represent the first direct observation of distinct morphological reorganization of an environmentally responsive hydrogel at internal fracture surfaces as a consequence of a phase transition.[22] This structural transition may have significant medical implications since certain pathological conditions that occur in native elastic fiber raise the transition temperature of the network above normal physiological temperature and would initiate a dramatic rearrangement of the elastic matrix mimicking our observations.[23]

Acknowledgment. The authors acknowledge the financial support of The Molecular Design Institute of The Georgia Institute of Technology, a Herman Frasch Foundation Grant from the American Chemical Society, and a NASA Research Agency grant (NAG8-1579). We also thank Professor Stevin Gehrke for helpful discussions and comments.

References and Notes

(1) Dumitrui, S.; Dumitrui-Medvichi, C. In *Polymeric Biomaterials*; Dumitrui, S., Ed.; Marcel Dekker: New York, 1994; pp 3−97.
(2) Gehrke, S. H.; Fisher, J. P.; Palasis, M.; Lund, M. E. *Ann. N. Y. Acad. Sci.* **1997**, *831*, 179−207.
(3) Apkarian, R. P.; Caran, K. L.; Robinson, K. A. *Microsc. Microanal.* **1999**, *5*, 197−207.
(4) A synthetic gene of approximately 3000 base pairs in length was isolated that encoded the protein polymer poly(**Lys-25**) as a C-terminal fusion to a decahistidine tag in pET-19b. Inducible expression of this gene in bacterial cultures of recombinant *Escherichia coli* strain BLR(DE3) afforded the elastin-mimetic protein polymer, which migrated as a single tight band at an apparent molecular mass of 94 kD as determined by 10−15% gradient denaturing polyacrylamide gel electrophoresis. Poly(**Lys-25**) was liberated from the leader sequence by cyanogen bromide cleavage, and was isolated as a colorless solid after concentration and lyophilization. The MALDI−TOF mass spectrum of poly(**Lys-25**) displayed a broadened peak centered at 80 645 kD, which most closely corresponded to a sequence comprising 39 repeats of **1** for poly(**Lys-25**) (expected mass = 81 095 kD).[9]
(5) McMillan, R. A.; Lee, T. A. T.; Conticello, V. P. *Macromolecules* **1999**, *32*, 3643−3648.
(6) Urry, D. W. *Prog. Biophys. Mol. Biol.* **1992**, *57*, 23−57.
(7) The phase diagram for a polydisperse protein polymer [Val-Pro-Gly-Pro-Gly)$_n$] (n_{avg} > 120) in aqueous solution has been mapped in the temperature−concentration plane, including the location of the coexistence and spinodal lines (Sciortino, F.; Prasad, K. U.; Urry, D. W.; Palma, M. U. *Biopolymers* **1993**, *33*, 743−752. Sciortino, F.; Urry, D. W.; Palma, M. U.; Prasad, K. U. *Biopolymers* **1990**, *29*, 1401−1407.).
(8) The elastin-mimetic protein polymer was cross-linked into a gel by treatment of a 5% (w/v) solution of the polypeptide in an aqueous buffer (50 mM phosphate pH 8.5) with a stoichiometrically equivalent amount of the water-soluble cross-linker bis(sulfosuccinimidyl)suberate. For reactions under aqueous conditions, the polypeptide was dissolved initially in the buffer at 4 °C, which is well below its transition temperature under the reaction conditions. The cross-linker was added at low temperature and the mixture warmed to 25 °C for the cross-linking reaction. Elastomeric networks based on repeat sequence **1** should contain cross-links at well-defined positions *in the limit of complete substitution* of the amino groups, although the actual degree of substitution, and hence, the upper limit of the cross-linking efficiency is approximately 88% for the hydrogel derived from poly(**Lys-25**).[9]
(9) McMillan, R. A.; Conticello, V. P. Submitted for publication in *J. Am. Chem. Soc.*
(10) Pasquali-Ronchetti, I.; Fornieri, C.; Baccarani-Contri, M.; Quaglino, D. *Ciba Found. Symp.* **1995**, *192*, 31−42.
(11) Mecham, R. P.; Heuser, J. E. In *Cell Biology of the Extracellular Matrix*; Hay, E. D., Ed.; Plenum Press: New York, 1991; pp 79−109.
(12) Pasquali-Ronchetti, I.; Alessandrini, A.; Baccarani-Contri, M.; Fornieri, C.; Mori, G.; Quaglino, D., Jr.; Valdrè, U. *Matrix Biol.* **1998**, *17*, 75−83.
(13) A detailed procedure has been reported for the topographic imaging of frozen, hydrated specimens that is summarized herein.[3] The specimens (ca. 20 μL of coacervate or gel) were mounted onto 3 mm gold planchets (Balzers BU 012 130T) and equilibrated at the desired temperature (either 4 or 40 °C) in an isothermal environmental cooler or heater. The liquid ethane cryogen was slowly condensed into the central well of a double dewar after the outer well had been filled with liquid nitrogen. The specimens were plunged into a pool of liquified ethane that was melted in the center of solidified ethane (ca. −183 °C). After 30 s, the carrier, which contained a coat of liquid ethane, was plunged into liquid nitrogen, at which time a dome-shaped crust of frozen ethane was formed on top of the carrier. The cryo-immobilized specimens were fractured with a precooled blade, and the fracture surface was rinsed with liquid nitrogen while the temperature of the specimen was equilibrated at −168 to −170 °C by the Oxford CT-3500 cryo-stage. The cryo-immobilized specimens (−160 °C) were sputter-coated with 1 nm layer of chromium metal[25] at a sputter pressure of 5×10^{-3} Torr in a Denton DV-602 magnetron sputter system. The specimens were imaged at a temperature of approximately −110 °C in the upper stage of a DS-130F field emission scanning electron microscope with an in-lens Oxford CT-3500 cryostage.
(14) Huang, L.; McMillan, R. A.; Apkarian, R. P.; Conticello, V. P.; Chaikof, E. L. Abstracts of the American Institute of Chemical Engineers (AIChE) National Meeting, Dallas, TX, Nov 1999.
(15) Bressan, G. M.; Pasquali-Ronchetti, I.; Fornieri, C.; Mattioli, F.; Castellani, I.; Volpin, D. *J. Ultrastruct. Mol. Struct. Res.* **1986**, *94*, 209−216.
(16) (a) Urry, D. W. *Angew. Chem., Int. Ed. Engl.* **1993**, *32*, 819−841. (b) Urry, D. W. *J. Prot. Chem.* **1988**, *7*, 1−34.
(17) Urry, D. W.; Shaw, R. G.; Prasad, K. U. *Biochem. Biophys. Res. Commun.* **1985**, *130*, 50−57.
(18) Thomas, G. J., Jr.; Prescott, B.; Urry, D. W. *Biopolymers* **1987**, *26*, 921−934.

(19) Urry, D. W.; Krishna, N. R.; Huang, D. H.; Trapane, T. L.; Prasad, K. U. *Biopolymers* **1989**, *28*, 819−833.
(20) Chang, D. K.; Venkatachalam, C. M.; Prasad, K. U.; Urry, D. W. *J. Biomol. Struct. Dyn.* **1989**, *6*, 851−858.
(21) Reiersen, H.; Clarke, A. R.; Rees, A. R. *J. Mol. Biol.* **1998**, *283*, 255−264.
(22) Atomic force microscopy has been employed recently for imaging of the surface roughness of mechanically constrained poly(*N*-isopropylacrylamide) hydrogels undergoing a similar temperature-dependent phase transition. (Suzuki, A.; Yamazaki, M.; Kobiki, Y. *J. Chem. Phys.* **1996**, *104*, 1751−1757. Suzuki, A.; Yamazaki, M.; Kobiki, Y.; Suzuki, H. *Macromolecules* **1997**, *30*, 2350−2354.).
(23) Urry, D. W.; Sugano, H.; Prasad, K. U.; Long, M. M.; Bhatnagar, R. S. *Biochem. Biophys. Res. Commun.* **1979**, *90*, 194−8.
(24) Matsuo, E. S.; Orkisz, M.; Sun, S.-T.; Li, Y.; Tanaka, T. *Macromolecules* **1994**, *27*, 6791−6796.
(25) Apkarian, R. P. *Scanning Microsc.* **1994**, *8*, 289−301.

MA991119Z